Journal of Molecular Spectroscopy 252 (2008) 190–197

Contents lists available at ScienceDirect

Journal of Molecular Spectroscopy

journal homepage: www.elsevier.com/locate/jms

New CW-CRDS measurements and global modeling of $^{12}C^{16}O_2$ absolute line intensities in the 1.6 μm region

B.V. Perevalov [a,b], A. Campargue [a,*], B. Gao [a,c], S. Kassi [a], S.A. Tashkun [b], V.I. Perevalov [b,*]

[a] Laboratoire de Spectrométrie Physique, UMR CNRS 5588, Université Joseph Fourier, BP 87, 38402 Saint Martin d'Hères Cedex, France
[b] Laboratory of Theoretical Spectroscopy, Institute of Atmospheric Optics, Siberian Branch, Russian Academy of Sciences, 1 Akademicheskii Avenue, 634055 Tomsk, Russia
[c] Hefei National Laboratory for Physical Sciences at Microscale, Department of Chemical Physics, University of Science and Technology of China, Hefei 230026, China

ARTICLE INFO

Article history:
Received 15 July 2008
In revised form 18 August 2008
Available online 30 August 2008

Keywords:
Molecular spectroscopy
Carbon dioxide
CO_2
Line intensities
Infrared
Global modeling
CW-CRDS
Cavity Ring Down Spectroscopy
Carbon Dioxide Spectroscopic Databank (CDSD)
HITRAN

ABSTRACT

Line intensities of $^{12}C^{16}O_2$ transitions have been measured by CW-Cavity Ring Down Spectroscopy in four wavenumber intervals near 1.6 μm. Intensity values of 952 transitions ranging from 1.10×10^{-28} to 4.94×10^{-25} cm/molecule were retrieved with an average accuracy of 4%. These transitions belong to a total of 30 bands corresponding to the $\Delta P = 9$ series of transitions. The achieved sensitivity (noise equivalent absorption $\alpha_{min} \sim 3 \times 10^{-10}$ cm^{-1}) allows lowering by more than two orders of magnitude the lower intensity values measured in the region. Comparison with the values included in the JPL database [R.A. Toth, L.R. Brown, C.E. Miller, V. Malathi Devi, D.C. Benner, J. Quant. Spectrosc. Radiat. Transf. 109 (2008) 906–921] shows residuals exceeding one order of magnitude for weak lines. The measured intensities together with a selection of experimental intensities available in the literature were used to extend and refine the set of effective dipole moment parameters for the $\Delta P = 9$ series of transitions of the principal isotopologue of carbon dioxide. The refined parameters allow reproducing, within the experimental uncertainties, the whole set of intensity measurements which extends over nearly six orders of magnitude (1.10×10^{-28}–6.12×10^{-23} cm/molecule). Combining the CW-CRDS line positions with the calculated line intensities, a line list has been generated for the whole 5851–7045 cm^{-1} region and is provided as Supplementary Material. The obtained effective dipole moment parameters have also been used to generate the $\Delta P = 9$ series of transitions included in the new version of the CDSD database. The comparison of the CDSD line intensities with the values provided by the HITRAN-2004 database shows discrepancies up to 80% for some of the bands while discrepancies up to three orders of magnitude are noted for the weakest bands included in the JPL database.

1. Introduction

The present contribution participates to the development of an improved version of the Carbon Dioxide Spectroscopic Databank (CDSD) [1,2]. It is devoted to the retrieval of experimental line intensities from new spectra recorded by CW-Cavity Ring Down Spectroscopy (CW-CRDS), and to the improvement of the theoretical description of the line intensities within the framework of the effective operators approach [3–8] for the principal isotopologue, $^{12}C^{16}O_2$, of carbon dioxide in the 1.6 μm region. The spectrum of carbon dioxide in this region is formed by the transitions belonging to the $\Delta P = 9$ series. According to the classification defined within the effective operators approach, the series of transitions are identified by the difference $\Delta P = P' - P''$, where $P = 2V_1 + V_2 + 3V_3$ is an integer that labels each polyad of vibrational basis states coupled by anharmonic and Coriolis resonance interactions [3]. V_i is the vibrational quantum number associated with the mode of vibration *i*.

The high sensitivity of the CW-CRDS spectrometer developed in Grenoble [9–14] makes possible to determine accurate values of line intensities down to 10^{-28} cm/molecule which is more than two orders of magnitude lower than the minimum value of the intensities previously measured in the region considered. The obtained results give the opportunity to discuss the recently elaborated JPL (Jet Propulsion Laboratory) carbon dioxide spectroscopic database [15]. This database is constructed on very precise measurements of line positions and line intensities by Fourier Transform Spectroscopy (FTS) [16–20]. However the authors of this database extrapolated their data down to a very low intensity cut-off of 4×10^{-30} cm/molecule while the minimum value of their measured line intensities was about 2×10^{-26} cm/molecule. As discussed in our recent publication devoted to the $^{13}C^{16}O_2$ isotopologue [21], this long range extrapolation leads to large residuals when compared to our observations both for line positions and line intensities. In the present study, we established a similar comparison for the principal isotopologue of carbon dioxide, $^{12}C^{16}O$.

* Corresponding authors. Fax: +33 4 76 63 54 95.
E-mail addresses: Alain.Campargue@ujf-grenoble.fr (A. Campargue), vip@lts.iao.ru (V.I. Perevalov).

0022-2852/$ - see front matter © 2008 Elsevier Inc. All rights reserved.
doi:10.1016/j.jms.2008.08.006

In the 1.6 μm region, the line intensities of the strong cold parallel bands dominating the spectrum have been measured by several authors using different experimental techniques: grating spectrometer [22], Fourier transform spectrometers [18,23–29] and diode laser absorption spectrometers [29–32]. The comparison of these measured line and band intensities has been detailed in Refs. [18,28]. The line intensities of the 3111*i*-01101 (i = 2, 3) and 01131-01101 hot bands have been measured in Ref. [28] and Ref. [26], respectively. In a recent JPL publication [18], accurate line intensity values were reported for the 00031-00001 and 3001*i*-00001 (i = 1–4) cold bands and for their respective hot bands. The line intensities of two cold perpendicular bands 1112*i*-00001 (i = 1, 2) were also obtained [18]. However, important experimental information were still missing for the determination of the effective dipole moment parameters of the $\Delta P = 9$ bands [8] which hampered a satisfactory modeling of the CO_2 absorption spectrum near 1.6 μm: no intensity measurements were available for the very weak 4110*i*-00001 (i = 1–5) and 2002*i*-01101 (i = 1–3) perpendicular bands and for the 2221*i*-00001 (i = 1–3) "forbidden" bands. These bands are showed on the lower panel of Fig. 1 together with the four spectral intervals chosen for new CW-CRDS measurements dedicated to these specific bands: 5851–5881, 5972–6035, 6373–6542 and 6622–6750 cm^{-1}. On the middle panel, the $^{12}C^{16}O_2$ overview spectrum as included in the new version of the CDSD [36] is presented for the 5800–6800 cm^{-1} region. The transitions measured by FTS in Ref. [18] are displayed in the upper

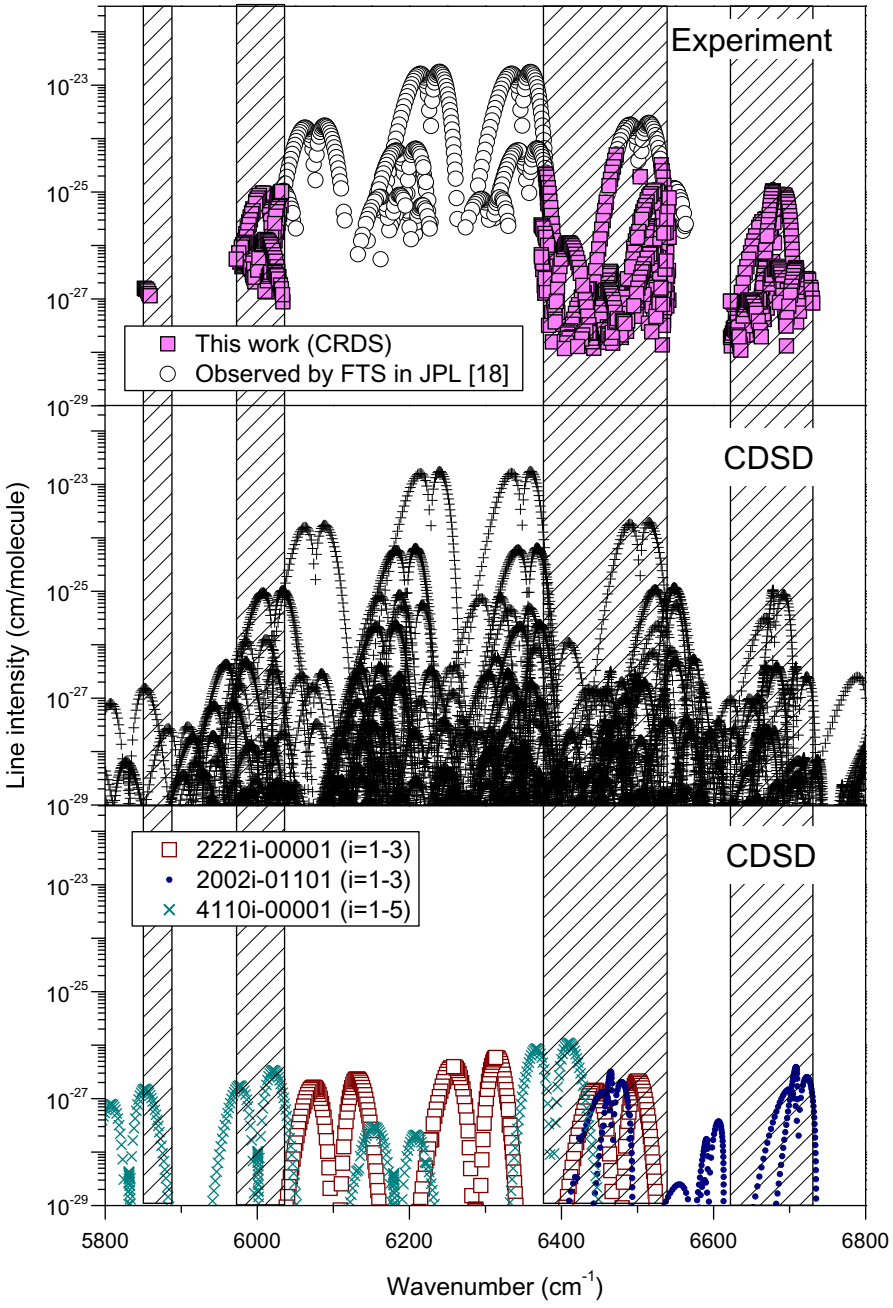

Fig. 1. Overview of the $^{12}C^{16}O_2$ measured line intensities and those provided by the most recent version of the CDSD database, in the 5800–6800 cm^{-1} spectral region. *Upper panel*: transitions whose line strengths were experimentally determined and used as input data for the dipole moment operators fit. The line strengths measured by CW-CRDS are highlighted with squares. *Middle panel*: CDSD database. *Lower panel*: the weak 4110*i*-00001 (i = 1–5), 2002*i*-01101 (i = 1–3) and 2221*i*-00001 (i = 1–3) bands as provided by the CDSD database. The CW-CRDS recordings were specifically dedicated to the line intensity measurements of these bands. The studied spectral intervals are indicated.

panel together with our new CW-CRDS measurements. Note that the line intensities of the bands of interest are lower than 10^{-26} cm/molecule, hence below the FTS detection threshold. The line positions analysis of the CW-CRDS spectrum in the whole 5850–7045 cm^{-1} range has been published in a separate contribution [34].

In the second part of the paper, our intensity values are gathered with measurements available in the literature in order to extend and refine the set of effective dipole moment parameters for the $\Delta P = 9$ series of transitions in $^{12}C^{16}O_2$.

2. Experimental details

The fibered CW-CRDS spectrometer and the procedure adopted for an accurate calibration of the wavenumber scale of the recorded spectra were described in Refs. [9–14,33]. The typical sensitivity (noise equivalent absorption $\alpha_{min} \sim 2\text{–}5 \times 10^{-10}$ cm^{-1}), the wide spectral coverage and the four to five decades linear dynamic range make it an ideal tool for high sensitivity absorption spectroscopy in the important atmospheric window of transparency around 1.5 μm. The full 5850–7045 cm^{-1} range can be investigated with the help of about 50 Distributed Feed-Back (DFB) diode lasers. The tuning range of each DFB laser is about 7 nm (~30 cm^{-1}) by temperature variation from −10 to 65 °C. In the present study, a total of 15 diode lasers were necessary to cover the four spectral intervals of interest (see Fig. 1). The typical ring down times were on the order of 60 μs but decreased to about 20 μs at 5900 cm^{-1}, which corresponds to the low energy limit of the high reflectivity region of the mirror set used. The ring down cell was filled with carbon dioxide in natural isotopic abundance (Fluka, stated purity >99.998%). The pressure, measured by a capacitance gauge, as well as the ringdown cell temperature, were monitored during the spectrum acquisition. The sample pressure was fixed to a value of 10.0 Torr and the room temperature was 296 ± 2 °K.

3. Line intensity retrieval

The integrated absorption coefficient I (in cm^{-2}) was obtained for each line using an interactive least squares multi-lines fitting program, which uses the Levenberg–Marquardt algorithm to minimize the deviation between the observed and calculated spectra. This procedure has been described in details in our previous paper [35]. The CO_2 line profile was assumed to be of Voigt type. The Gaussian line widths were fixed to the values calculated for the Doppler broadening, according to the measured temperature and masses of the CO_2 isotopologues. The Lorentzian line widths were calculated as the product of the sample pressure by the self-broadening coefficients provided in the HITRAN database [37]. Because the laser line width is much smaller than the Doppler width, the contribution of the apparatus function can be neglected. The baseline was modelled by a linear or a quadratic function of the wavenumber. The lines due to water vapor (H_2O and HDO), present as an impurity in the sample, were also fitted. Their Gaussian line widths were fixed to their theoretical values while the Lorentzian component was calculated using the H_2O broadening coefficients due to collisions with CO_2 [38]. The position and integrated absorbance of each line and the baseline coefficients were provided by the fitting procedure. Fig. 2 illustrates the large dynamics achieved on the measurement of the line intensities and the quality of the spectrum reproduction.

The absolute line intensity or integrated absorption coefficient per pressure unit $\tilde{S}$ (in $cm^{-2}\,atm^{-1}$) was deduced from the integrated absorption coefficient I using the equation:

$$\tilde{S} = \frac{I}{P}, \tag{1}$$

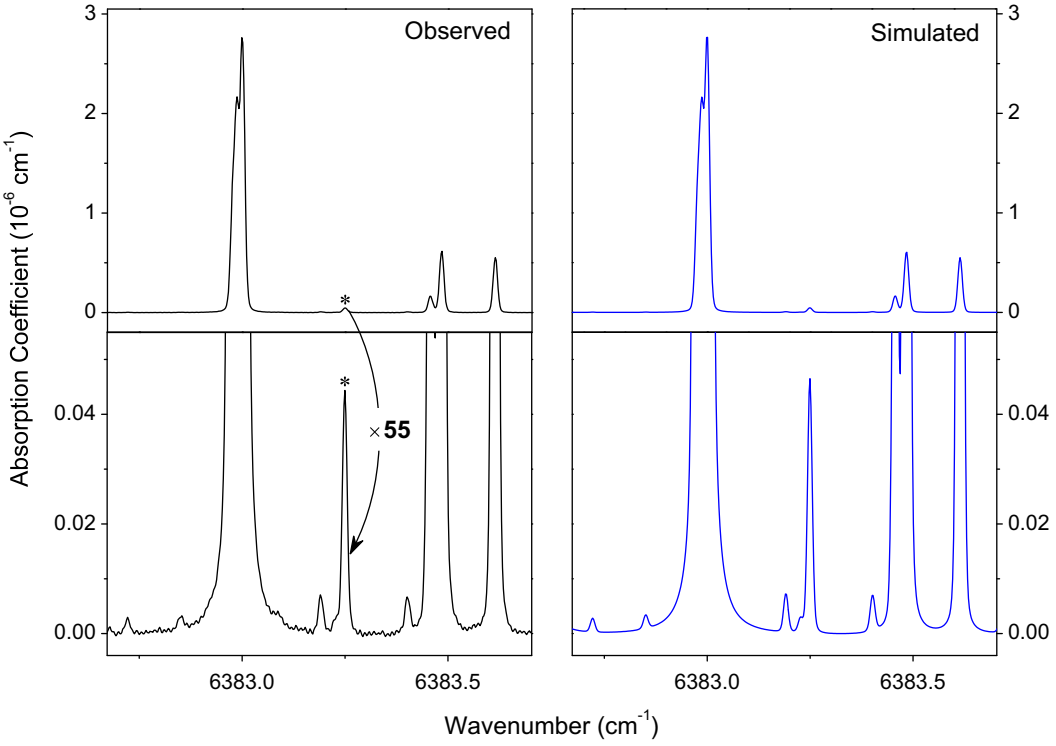

Fig. 2. Comparison of the CW-CRDS spectrum of carbon dioxide (P = 13.3 hPa) in natural abundance (left hand) with a simulated spectrum (right hand). In the lower panels, the ordinate scale has been amplified by a factor of 55 in order to visualize lines which are 1000 times weaker than the strongest lines of the presented region. The simulated spectrum was obtained as a sum of Voigt profiles whose parameters were determined with an interactive least-squares multi-lines fitting program (see text).

where P is the $^{12}C^{16}O_2$ partial pressure (in atm). Each $\widetilde{S}$ value was then converted to the absorption line intensity $S(T_0)$ (in cm/molecule) according to the following expression:

$$S(T_0) = \frac{1}{N_L}\frac{T_0}{273.15}\widetilde{S}, \quad (2)$$

where $T_0 = 296$ K and $N_L = 2.68676 \times 10^{19}$ molecule cm^{-3} atm^{-1} is the Loschmidt number.

The relative concentration of water vapour contaminating the CO_2 sample was retrieved from the observed H_2O line intensities in different spectral regions. The obtained values were always lower than 2×10^{-3} and the H_2O contribution to the total pressure value was then neglected.

Taking into account the transitions due to the different CO_2 isotopologues ($^{12}C^{16}O_2$, $^{13}C^{16}O_2$, $^{16}O^{12}C^{18}O$, $^{16}O^{12}C^{17}O$, $^{16}O^{13}C^{18}O$) [34], the lines due H_2O and HDO present as an impurity, the existence of overlapping spectral regions recorded with successive diode lasers, the total number of fitted line profiles was about 4600. After averaging of the line intensities of the same line determined from different spectra, 1572 line intensity values ranging from 1.53×10^{-29} to 4.94×10^{-25} cm/molecule were obtained for $^{12}C^{16}O_2$. Note that the strongest lines ($S > 5 \times 10^{-25}$ cm/molecule) which were saturated on the spectrum were not fitted since the accurate line intensities of these lines were measured in Ref. [18]. We fixed the lower line intensity cutoff to a value of 10^{-28} cm/molecule and removed from the list 214 line intensities below this value because of insufficient accuracy. In addition, 406 intensity values of the lines with unsatisfactory line profile reproduction (blended lines or incorrect baseline) were excluded. The fitting error was estimated to be 3% or better for well-isolated lines. The larger errors were mainly due to the uncertainty on the baseline determination which became more important for the weak lines. The final set, thus containing 952 $^{12}C^{16}O_2$ line intensities, was used as input data to the fit of the effective dipole moment parameters (see below). Taking into account the line profile fitting errors and the uncertainties on the temperature (±2 K) and pressure (±0.5%), we estimated that the accuracy of these 952 line intensities should be 4% or better for most of the lines and at most 7% for the weakest and strongly blended lines.

Fig. 3 shows the comparison of our line intensities with those provided in the JPL database [15] and with those *measured* at JPL [18]. A good agreement is noted with the *measured* line intensities whereas the residuals between our measurements and the line intensities extrapolated (or theoretically predicted) at JPL can exceed one order of magnitude. The major reason of these disagreements is that simple empirical expansions of the transition moment squared in terms of vibrational moment squared and Herman–Wallis parameters, as used for the transitions beyond JPL observations, cannot be applied in the case of perturbed bands. Moreover, the choice of a low intensity cutoff (4×10^{-30} cm/molecule) forces long range extrapolations on the angular momentum quantum number J. Such extrapolations are particularly hazardous as occurrences of perturbations are expected to increase with J values and may be pronounced.

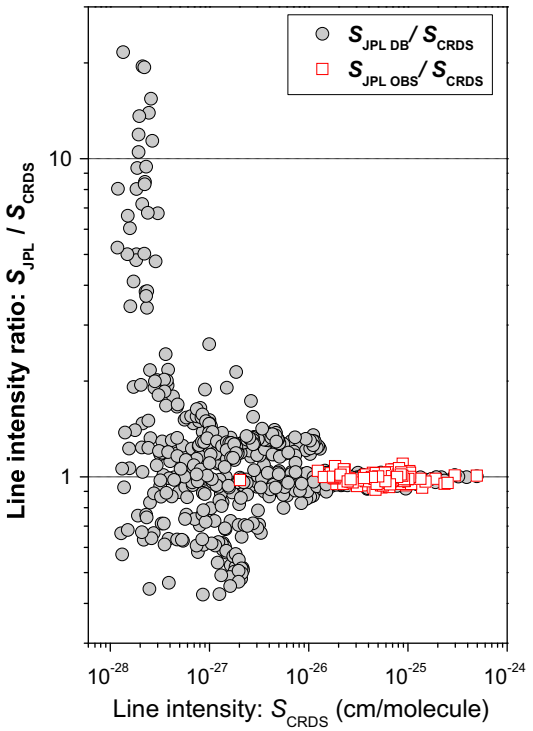

Fig. 3. Ratio of the $^{12}C^{16}O_2$ line intensities provided in the JPL database [15] to the ones measured by CW-CRDS, plotted as a function of the CW-CRDS intensity values. The JPL database includes measured values [18] and extrapolated (or calculated) values; the corresponding ratios are plotted with open squares and full circles, respectively.

4. Modeling and fitting of the line intensities

4.1. Theoretical approach

Using the effective operators approach, it is possible to model simultaneously the line intensities of the cold and hot bands belonging to the same series of transitions. For the reader's convenience, we briefly recall this approach which has been presented in several of our papers [6–8]. As a result of the approximate relations between the harmonic frequencies

$$\omega_1 \approx 2\omega_2, \quad \omega_3 \approx 3\omega_2 \quad (3)$$

the effective Hamiltonian [3–5,39] globally describing the line positions of carbon dioxide is formulated with the assumption that the vibration–rotation energy levels can be separated in polyads. The effective Hamiltonian takes into account all resonance interactions between vibration–rotation states belonging to the same polyad, up to the sixth-order of the perturbation theory. The polyad model of the effective Hamiltonian is very satisfactory for carbon dioxide, especially for the symmetric species. As mentioned in the Introduction the polyads can be identified with the label

$$P = 2V_1 + V_2 + 3V_3, \quad (4)$$

where V_i are vibrational quantum numbers.

Within the effective operators approach, the square of the transition dipole moment of a vibration–rotation transition $P'N'J'\varepsilon' \leftarrow PNJ\varepsilon$ is given by [6–8]

$$W_{P'N'J'\varepsilon'\leftarrow PNJ\varepsilon} = (2J+1)\left|\sum_{V_1V_2\ell_2V_3}\sum_{\substack{2\Delta V_1+\Delta V_2+3\Delta V_3=\Delta P \\ \Delta\ell_2=0,\pm1,\pm2,\ldots}} {}^{J}C^{V_1V_2\ell_2V_3}_{PN\varepsilon}\, {}^{J'}C^{V_1+\Delta V_1V_2+\Delta V_2\ell_2+\Delta\ell_2V_3+\Delta V_3}_{P'N'\varepsilon'} M^{|\Delta\ell_2|}_{\Delta V} \times \sqrt{f^{\Delta\ell_2}_{\Delta V}(V,\ell_2)(1+\delta_{\ell_2,0}+\delta_{\ell_{2'},0}-2\delta_{\ell_2,0}\delta_{\ell_{2'},0})}\,\Phi_{\Delta J,\Delta\ell_2}(J,\ell_2) \times \left(1+\sum_i \kappa^{\Delta V}_i V_i + F^{\Delta\ell_2}_{\Delta V}(J,\ell_2)\right)\right|^2. \quad (5)$$

where $\delta_{i,j}$ is the Kronecker symbol and ${}^{J}C^{V_1V_2\ell_2V_3}_{PN\varepsilon}$ stands for the expansion coefficient determining the eigenfunction of the lower state,

$$\Psi^{\mathrm{eff}}_{PNJ\varepsilon} = \sum_{2V_1+V_2+3V_3=P,\ell_2} {}^{J}C^{V_1V_2\ell_2V_3}_{PN\varepsilon} \mid V_1V_2 \mid \ell_2 \mid V_3J\varepsilon\rangle. \quad (6)$$

The summation runs over all states within the polyad involved. The definition of the Wang-type basis functions $|V_1V_2|\ell_2|V_3J\varepsilon\rangle$ is given, for example, in Ref. [6]. In the same way, ${}^{J'}C^{V_1V_2\ell_2V_3}_{P'N'\varepsilon'}$ stands for the expansion coefficient within the upper-state polyad. The functions $\Phi_{\Delta J\Delta\ell_2}(J,\ell_2)$ for $\Delta\ell_2 = 0, \pm1$ are equal to the Clebsh–Gordon coefficients $(1\Delta\ell_2 J\ell_2|(J+\Delta J)(\ell_2+\Delta\ell_2))$, related to the Hönl–London factors by the equation

$$(1\Delta\ell_2 J\ell_2 \mid (J+\Delta J)(\ell_2+\Delta\ell_2))|^2 = \frac{L^{\Delta\ell_2}_{\Delta J}}{2J+1}. \quad (7)$$

The $f^{\Delta\ell_2}_{\Delta V}(V,\ell_2)$ functions are listed in Table 1 of Ref. [6] for small values of the quantum number differences ΔV. The Herman–Wallis-type functions $F^{\Delta\ell_2}_{\Delta V}(J,\ell_2)$ appearing in Eq. (5) are given in Ref. [7]. Here, we present only the terms used in this paper:

$$F^{\Delta\ell_2}_{\Delta V}(J,\ell_2) = b^{\Delta V}_J m \quad (8)$$

for the $\Delta\ell_2 = 0$ matrix elements,

$$F^{\Delta\ell_2}_{\Delta V}(J,\ell_2) = -\frac{1}{2}b^{\Delta V}_J(2\ell_2\Delta\ell_2+1) \quad (9)$$

for the $\Delta J = 0$, $\Delta\ell_2 = \pm1$ matrix elements, and

$$F^{\Delta\ell_2}_{\Delta V}(J,\ell_2) = -\frac{1}{2}b^{\Delta V}_J(2\ell_2\Delta\ell_2+1) + b^{\Delta V}_J m \quad (10)$$

for $\Delta J = \pm1$, $\Delta\ell_2 = \pm1$ matrix elements. Here $m = -J$ for P-branch and $m = J+1$ for R-branch.

The $M^{|\Delta\ell_2|}_{\Delta V}$, $\kappa^{\Delta V}_i$ ($i = 1$–3), and $b^{\Delta V}_J$ parameters of the effective dipole moment matrix elements involved in Eqs. (5) and (8)–(10) allow the simultaneous description of the intensities of all the lines of cold and hot bands belonging to a series of transitions characterized by a given value of ΔP. These parameters were fitted to the observed line intensities.

4.2. Line intensities fitting

Using the above approach, we have performed the least-squares fitting of the line intensities set obtained by gathering the CW-CRDS results with selected intensity data reported in the literature for the $\Delta P = 9$ series of transitions [18,22,26,28–31]. The selection has been performed on the basis of the comparative analysis of all published line intensities following the results of Refs. [18,28]. The sources in which the line intensities differ considerably from those confirmed by several authors were not included in the fit. In general, these discarded data came from rather old publications. Because of the comparative analysis performed in Refs. [18,28], in several cases, only part of the data presented in a given source were included into the fit. In the fitting process, some evident outliers were excluded from the input file. Table 1 presents the sources of the input data and the corresponding percentage of line intensities included in the fit. The values of the expansion coefficients ${}^{J}C^{V_1V_2\ell_2V_3}_{PN\varepsilon}$ of the eigenfunctions have been obtained from the global fit of the effective Hamiltonian parameters to the observed line positions. The initial set of effective Hamiltonian parameters taken from Ref. [10] was slightly refined using new observations [34]. The partition functions $Q(T)$ and nuclear statistical weights were taken from Ref. [40].

The aim of the fitting process is to minimize the dimensionless weighted standard deviation χ, defined according to the usual formula,

$$\chi = \sqrt{\frac{\sum_{i=1}^{N}\left(\frac{S_i^{\mathrm{obs}}-S_i^{\mathrm{calc}}}{\delta_i}\right)^2}{(N-n)}}, \quad (11)$$

where S_i^{obs} and S_i^{calc} are, respectively, the observed and calculated values of the intensity for the ith line; $\delta_i = \frac{S_i^{\mathrm{obs}}\sigma_i}{100\%}$, where σ_i is the measurement error of the i-th line in %, N is the number of fitted line intensities, and n is the number of adjusted parameters. To characterize the quality of a fit, we also use the root mean square (RMS) deviation, defined according to the equation

$$\mathrm{RMS} = \sqrt{\frac{\sum_{i=1}^{N}\left(\frac{S_i^{\mathrm{obs}}-S_i^{\mathrm{calc}}}{S_i^{\mathrm{obs}}}\right)^2}{N}} \times 100\%. \quad (12)$$

The line intensities were weighted according to their assumed uncertainties σ_i which are based on the declared absolute accuracies. When, in a respective source, each individual line was supplied with its uncertainty, this uncertainty was used in the fit. Otherwise, we used assumed uncertainty values as given in Table 1.

The fitting results presented in Tables 1 and 2 show that, in average, our fitted set of effective dipole moment parameters reproduces the line intensities from all involved experimental

Table 1
Experimental data and results of the global fits of the line intensities

Reference	Abundance	Accuracy (%)	Assumed uncertainty (%)	N[a]	%N[b]	RMS[c] (%)
Toth et al. [22]	0.9842	4	4	74	57.2	2.6
Johns et al. [26]	0.9842	2–4		150	94.8	2.2
Henningsen and Simonsen [30]	0.9842	2–12		29	69.0	2.5
Pouchet et al. [31]	0.9842	1.5–3		13	100	1.3
Boudjaadar et al. [28]	1.0	3–5	3, 5[d]	269	100	2.0
Régalia-Jarlot et al. [29]	0.9842	1.5–2	2	97	100	1.0
Toth et al. [18]	0.9842, 0.9952	0.5–3	2	808	99.0	2.9
This work	0.9842	2–7	4	928	97.5	3.4

[a] N—number of the fitted line intensities from a given source.
[b] %N—percentage of the line intensities of a given source included into the fit.
[c] RMS—root mean squares of the residuals for a given source.
[d] 3% for the cold bands, 5% for the hot bands.

Table 2
Summary of the line intensity fit for the $\Delta P = 9$ series of transitions in $^{12}C^{16}O_2$

Number of line intensities	Number of bands	$J_{\max}$	$S_{\min}$[a]	$S_{\max}$[a]	χ	RMS (%)	n[b]
2368	40	84	1.10×10^{-28}	6.12×10^{-23}	1.05	2.9	19

[a] $S_{\min}$ and $S_{\max}$ (in cm/molecule) are the minimum and maximum line intensity values included into the fit.
[b] n is the number of adjusted parameters.

sources within their uncertainties. The values of the fitted parameters are listed in Table 3. Fig. 4 presents the variation of the residuals between the observed and calculated line intensities versus the line intensity values. It illustrates the nearly six orders of magnitude dynamics of the line intensities covered by the input data and the consistency of the line intensities obtained from different experimental sources.

As a test of the validity of our model, it is worth emphasizing that no $|\Delta\ell_2| > 1$ effective dipole moment parameters were necessary to describe the line intensities of the $|\Delta\ell_2| > 1$ "forbidden" bands. These "forbidden" bands borrow most of their intensities from "allowed" bands *via* ℓ-type and anharmonic + ℓ-type interactions which are taken into account by our effective Hamiltonian model. The $|\Delta\ell_2| > 1$ effective dipole moment parameters give negligible contributions to the intensities such that no corresponding parameters were included in our fitting. As an example, Fig. 5 shows that the line intensities of the very weak 22211-00001 "forbidden" band studied in this work, are satisfactorily reproduced with our set of parameters.

Table 3
Effective dipole moment parameters for $\Delta P = 9$ series of transitions in $^{12}C^{16}O_2$

Parameter[a]	ΔV_1	ΔV_2	ΔV_3	$\Delta\ell_2$	Value	Order
M	0	0	3	0	0.31068(34)[b]	10^{-3}
κ_1	0	0	3	0	−20.52(39)	10^{-2}
κ_2	0	0	3	0	2.52(10)	10^{-2}
M	3	0	1	0	−0.26621(13)	10^{-3}
κ_1	3	0	1	0	−0.21(11)	10^{-2}
κ_2	3	0	1	0	−0.318(56)	10^{-2}
b_J	3	0	1	0	0.264(11)	10^{-3}
M	2	2	1	0	0.24145(57)	10^{-4}
M	1	4	1	0	−0.1216(15)	10^{-5}
M	0	6	1	0	0.339(28)	10^{-7}
M	1	1	2	1	0.21783(18)	10^{-4}
b_J	1	1	2	1	3.616(41)	10^{-3}
M	0	3	2	1	−0.9378(62)	10^{-6}
b_J	0	3	2	1	11.58(30)	10^{-3}
M	4	1	0	1	−0.288(32)	10^{-6}
b_J	4	1	0	1	80.6(38)	10^{-3}
M	3	3	0	1	0.57(12)	10^{-7}
b_J	3	3	0	1	99.9(63)	10^{-3}
M	2	−1	2	1	0.1947(58)	10^{-5}

[a] The parameters M are given in *Debye* while the b_J and κ_i parameters are dimensionless. Only relative signs of M parameters within a given series of transitions are determined.

[b] The numbers in parentheses are one standard deviation in units of the last quoted digit.

5. New line lists and their comparison with previous databases

By combining the present results and those from our recent paper relative to the line positions in the full 5851–7045 cm^{-1} range [10,34], we have generated two line lists for the $^{12}C^{16}O_2$ isotopologue of carbon dioxide in the 1.6 μm region. The first one is the CW-CRDS "experimental" line list, which was constructed by associating calculated line intensities to the measured line positions. It includes 5604 transitions belonging to 94 bands and is provided as

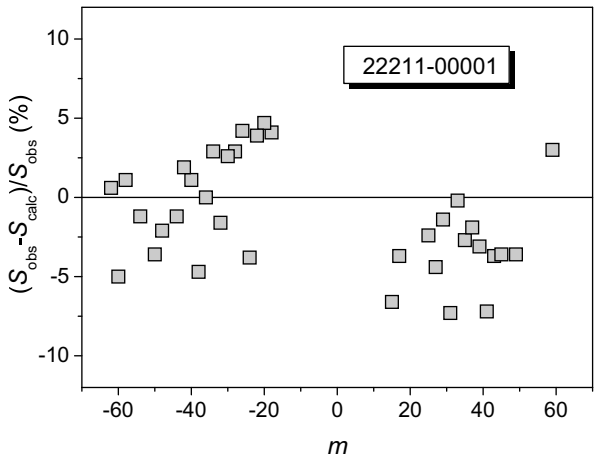

Fig. 5. Residuals between the observed and calculated line intensities of the 22211-00001 "forbidden" band centered at 6474.532 cm^{-1} versus the rotational quantum number m (where $m = -J$ and $m = J + 1$ for P and R branches, respectively). Note that the corresponding line intensities are very small, ranging from 1.5×10^{-28} to 2.2×10^{-27} cm/molecule.

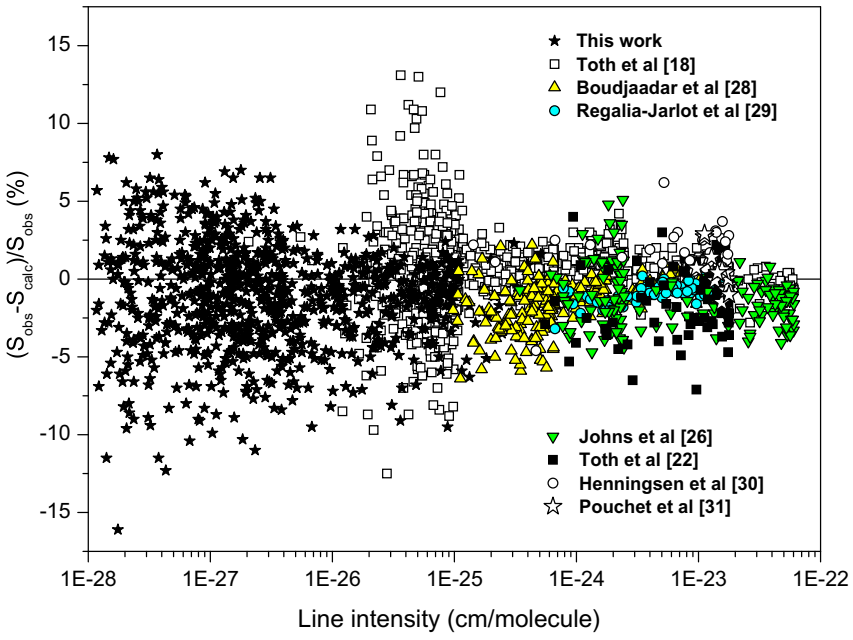

Fig. 4. Residuals between the observed and calculated line intensities in the 1.6 μm region versus the line intensity values. A different symbol is used for each experimental work.

Supplementary Material. The line intensities were calculated using the above dipole moment parameters. The second line list is the one included into the new version of the CDSD [36]. Both line positions and line intensities were calculated in the frame of the polyad model of effective Hamiltonian and respective effective dipole moment operator. The intensity cutoff was fixed to a value of 10^{-30} cm/molecule, i.e. significantly below the CW-CRDS sensitivity. It consists of 20 161 lines belonging to 256 bands.

The detailed comparison of the line positions contained in these line lists with those from HITRAN, GEISA and JPL databases has been presented in our previous paper [34]. Here, we focus on the comparison of the line intensities. In Section 2, it has been shown that, in the JPL database, extrapolations between 5×10^{-26} cm/molecule (corresponding to the JPL sensitivity by FTS) and 1×10^{-28} cm/molecule (corresponding to our CW-CRDS measurements), are responsible for important deviations up to a factor of 10. Such disagreements are expected to increase when extrapolating down to 4×10^{-30} cm/molecule which is the intensity cutoff adopted in the JPL database. Indeed, Fig. 6 shows that the ratios of the CDSD intensities [36] to the (mostly extrapolated) JPL intensities [15] range from 0.004 to 1000, reflecting the poor extrapolation capabilities of the empirical model used in Ref. [15].

The comparison of our calculated line intensities with those contained in the current version of the HITRAN database [37] shows rather large residuals for some of the hot bands and weak cold bands (see Fig. 7). The HITRAN intensities for these bands were calculated using the Direct Numerical Diagonalization (DND) approach [41]. We also note significant residuals even for the strongest bands, 30012-00001 and 30013-00001, in particular for high values of the angular momentum quantum number J. This is due to the fact that the HITRAN line intensities for these two bands are based on measurements [24,25] with poor accuracies for high J values. Our observations agree with the discussion included in Ref. [18].

6. Conclusion

Line intensities of the principal isotopologue of carbon dioxide, $^{12}C^{16}O_2$, have been measured by CW-Cavity Ring Down Spectroscopy in four wavenumber intervals near 1.6 μm. We chose to investigate the intervals corresponding to the very weak 4110i-00001 (i = 1–5) and 2002i-01101 (i = 1–3) perpendicular bands and to the 2221i-00001 (i = 1–3) "forbidden" bands, for which no experimental intensities were available. These measurements resulted in the determination of 952 intensities of transitions belonging to a total of 30 bands. The line intensities of 23 of these bands were measured for the first time. The intensity values ranged from 1.10×10^{-28} to 4.94×10^{-25} cm/molecule and the absolute accuracy varied from 2% for the strongest lines to 7% for the weakest lines and was estimated to be, in average, around 4%. Our measurements lowered by two orders of magnitude the minimum intensity values previously measured in the considered spectral region. They are in good agreement with the JPL experimental values [18] for line intensities higher than 5×10^{-26} cm/molecule.

The CW-CRDS line intensities and those selected from the literature have been used to fit the effective dipole moment parameters for the $\Delta P = 9$ series of transitions. The CW-CRDS measurements have allowed determining some important missing effective dipole moment parameters and refining the other parameters. In average, the new set of effective dipole moment parameters and refined set of effective Hamiltonian parameters reproduce all measured line intensities of the $\Delta P = 9$ series of transitions within the experimental uncertainties. They have been used to generate the line list for the $\Delta P = 9$ series of transitions in $^{12}C^{16}O_2$ with an intensity cutoff

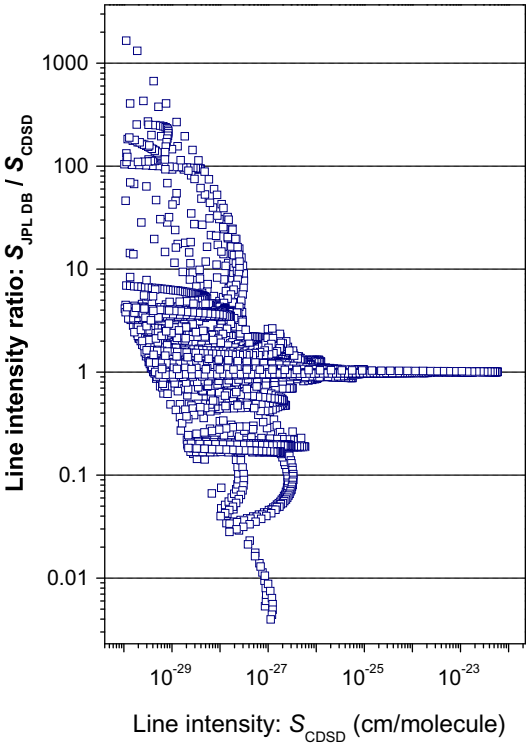

Fig. 6. Ratio of the $^{12}C^{16}O_2$ line intensities given in the JPL database [15] to the ones provided in the CDSD database [36] (extrapolated or calculated) plotted as a function of the CDSD line intensities. Note the logarithmic scale adopted for the ordinate scale.

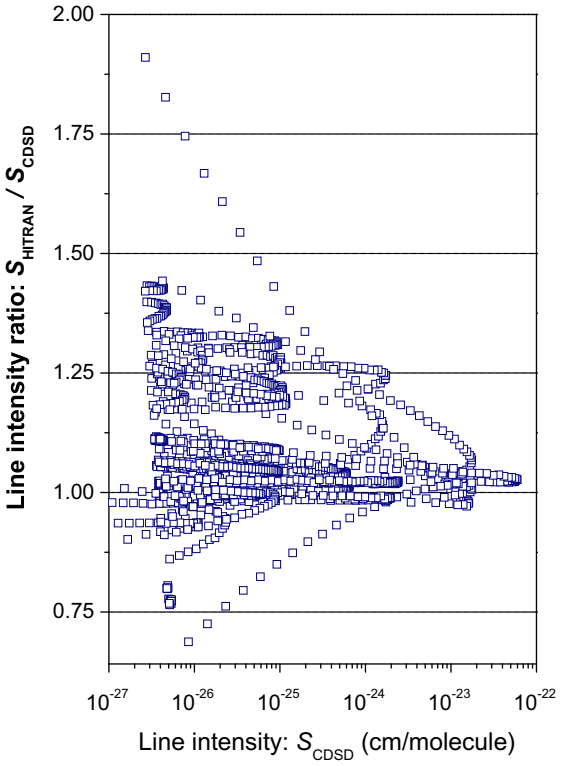

Fig. 7. Ratio of the $^{12}C^{16}O_2$ line intensities provided in the HITRAN database [37] to the ones given in the CDSD database [36], plotted as a function of the CDSD line intensities. Note the logarithmic scale adopted for the ordinate scale.

fixed to a value of 10^{-30} cm/molecule. This line list is now included in the new version of the CDSD [36].

Important discrepancies between our measurements and the intensity values provided in the recent JPL database [15] exist for the weak lines. The simple empirical equations adopted in Ref. [15] in order to extrapolate line intensities beyond the JPL observations are responsible of these deviations as such extrapolations towards high J values are not valid in the case of perturbed bands.

Acknowledgments

B.P. thanks the European research network QUASAAR (MRTN-CT-2004-512202) for his fellowship. This work is jointly supported by a collaborative projects between CNRS-France and RFBR-Russia, between CNRS and CAS-China (PICS Grant No. 3359), and between RFBR-Russia and NSFC–China (Grant No. 06-05-39016). The support from the "Programme National LEFE (CHAT) INSU-CNRS" is acknowledged.

Appendix A. Supplementary data

Supplementary data for this article are available on ScienceDirect (www.sciencedirect.com) and as part of the Ohio State University Molecular Spectroscopy Archives (http://library.osu.edu/sites/msa/jmsa_hp.htm). Supplementary data associated with this article can be found, in the online version, at doi:10.1016/j.jms.2008.08.006.

References

[1] S.A. Tashkun, V.I. Perevalov, J.-L. Teffo, A.D. Bykov, N.N. Lavrentieva, CDSD-296, The carbon dioxide spectroscopic databank: version for atmospheric applications, XIV Symposium on High Resolution Molecular Spectroscopy, Krasnoyarsk, Russia, July 6–11, 2003.
[2] S.A. Tashkun, V.I. Perevalov, J.-L. Teffo, A.D. Bykov, N.N. Lavrentieva, J. Quant. Spectrosc. Radiat. Transf. 82 (2003) 165–196.
[3] A. Chédin, J. Mol. Spectrosc. 76 (1979) 430–491.
[4] J.-L. Teffo, O.N. Sulakshina, V.I. Perevalov, J. Mol. Spectrosc. 156 (1992) 48–64.
[5] S.A. Tashkun, V.I. Perevalov, J.-L. Teffo, L.S. Rothman, V.G. Tyuterev, J. Quant. Spectrosc. Radiat. Transf. 60 (1998) 785–801.
[6] V.I. Perevalov, E.I. Lobodenko, O.M. Lyulin, J.-L. Teffo, J. Mol. Spectrosc. 171 (1995) 435–452.
[7] J.-L. Teffo, O.M. Lyulin, V.I. Perevalov, E.I. Lobodenko, J. Mol. Spectrosc. 187 (1998) 28–41.
[8] S.A. Tashkun, V.I. Perevalov, J.-L. Teffo, V.G. Tyuterev, J. Quant. Spectrosc. Radiat. Transf. 62 (1999) 571–598.
[9] Y. Ding, P. Macko, D. Romanini, V.I. Perevalov, S.A. Tashkun, J.-L. Teffo, S.-M. Hu, A. Campargue, J. Mol. Spectrosc. 226 (2004) 146–160.
[10] Z. Majcherova, P. Macko, D. Romanini, V.I. Perevalov, S.A. Tashkun, J.-L. Teffo, A. Campargue, J. Mol. Spectrosc. 230 (2005) 1–21.
[11] B.V. Perevalov, S. Kassi, D. Romanini, V.I. Perevalov, S.A. Tashkun, A. Campargue, J. Mol. Spectrosc. 238 (2006) 241–255.
[12] B.V. Perevalov, S. Kassi, D. Romanini, V.I. Perevalov, S.A. Tashkun, A. Campargue, J. Mol. Spectrosc. 241 (2007) 90–100.
[13] P. Macko, D. Romanini, S.N. Mikhailenko, O.V. Naumenko, S. Kassi, A. Jenouvrier, V.G. Tyuterev, J. Mol. Spectrosc. 227 (2004) 90–108.
[14] S.N. Mikhailenko, W. Le, S. Kassi, A. Campargue, J. Mol. Spectrosc. 244 (2007) 170–178.
[15] R.A. Toth, L.R. Brown, C.E. Miller, V. Malathy Devi, D.C. Benner, J. Quant. Spectrosc. Radiat. Transf. 109 (2008) 906–921.
[16] C.E. Miller, L.R. Brown, J. Mol. Spectrosc. 228 (2004) 329–354.
[17] C.E. Miller, M.A. Montgomery, R.M. Onorato, C. Johnstone, T.P. McNicholas, B. Covaric, L.R. Brown, J. Mol. Spectrosc. 228 (2004) 355–374.
[18] R.A. Toth, L.R. Brown, C.E. Miller, V.M. Devi, D.C. Benner, J. Mol. Spectrosc. 239 (2006) 221–242.
[19] R.A. Toth, C.E. Miller, L.R. Brown, V. Malathy Devi, D.C. Benner, J. Mol. Spectrosc. 243 (2007) 43–61.
[20] R.A. Toth, C.E. Miller, L.R. Brown, V. Malathy Devi, D.C. Benner, J. Mol. Spectrosc. 251 (2008) 64–89.
[21] A. Campargue, B.V. Perevalov, J. Quant. Spectrosc. Radiat. Transf. 109 (2008) 2261–2271.
[22] R.A. Toth, R.H. Hunt, E.K. Plyer, J. Mol. Spectrosc. 38 (1971) 107–117.
[23] C.B. Suarez, E.P.J. Valero, J. Quant. Spectrosc. Radiat. Transf. 19 (1977) 569–578.
[24] E.P.J. Valero, C.B. Suarez, J. Quant. Spectrosc. Radiat. Transf. 19 (1977) 579–590.
[25] C.B. Suarez, E.P.J. Valero, J. Mol. Spectrosc. 71 (1978) 46–63.
[26] J.W.C. Johns, Z. Lu, F. Thibault, R. Le Doucen, Ph. Arcas, Ch. Boulet, J. Mol. Spectrosc. 159 (1993) 259–264.
[27] M. Fukabori, T.A. Aoki, T.E. Aoki, H. Ishida, T. Watanabe, Adv. Space Res. 25 (2000) 985–988.
[28] D. Boudjaadar, J.Y. Mandin, V. Dana, N. Picqé, G. Guelachvili, J. Mol. Spectrosc. 236 (2006) 158–167.
[29] L. Régalia-Jarlot, V. Zéninari, B. Parvitte, A. Grossel, X. Thomas, P. Von der Heyden, G. Durry, J. Quant. Spectrosc. Radiat. Transf. 101 (2006) 325–338.
[30] J. Henningsen, H. Simonsen, J. Mol. Spectrosc. 203 (2000) 16–27.
[31] I. Pouchet, V. Zéninari, B. Parvitte, G. Durry, J. Quant. Spectrosc. Radiat. Transf. 83 (2004) 619–628.
[32] T. Hikida, K.M.T. Yamada, M. Fukabori, T. Aoki, J. Mol. Spectrosc. 232 (2005) 202–212.
[33] J. Morville, D. Romanini, A.A. Kachanov, M. Chenevier, Appl. Phys. D78 (2004) 465–476.
[34] B.V. Perevalov, S. Kassi, V.I. Perevalov, S.A. Tashkun, A. Campargue, J. Mol. Spectrosc. 252 (2008) 143–159.
[35] B.V. Perevalov, T. Deleporte, A.W. Liu, S. Kassi, A. Campargue, J. Vander Auwera, S.A. Tashkun, V.I. Perevalov, J. Quant, Spectrosc. Radiat. Transf. 109 (2008) 2009–2026.
[36] S.A. Tashkun, V.I. Perevalov, ftp://ftp.iao.ru/pub/CDSD-2008/.
[37] L.S. Rothman, D. Jacquemart, A. Barbe, D. Chris Benner, M. Birk, L.R. Brown, M.R. Carleer, C. Chackerian Jr., K. Chance, V. Dana, V.M. Devi, J.-M. Flaud, R.R. Gamache, A. Goldman, J.-M. Hartmann, K.W. Jucks, A.G. Maki, J.Y. Mandin, S.T. Massie, J. Orphal, A. Perrin, C.P. Rinsland, M.A.H. Smith, J. Tennyson, R.N. Tolchenov, R.A. Toth, J. Vander Auwera, P. Varanasi, G. Wagner, J. Quant. Spectrosc. Radiat. Transf. 96 (2005) 139–204.
[38] N.N. Lavrentieva, private communication.
[39] S.A. Tashkun, V.I. Perevalov, J.-L. Teffo, M. Lecoutre, T.R. Huet, A. Campargue, D. Bailly, M.P. Esplin, J. Mol. Spectrosc. 200 (2000) 162–176.
[40] J. Fischer, R.R. Gamache, A. Goldman, J. Quant. Spectrosc. Radiat. Transf. 82 (2003) 401–412.
[41] R.B. Wattson, L.S. Rothman, J. Quant. Spectrosc. Radiat. Transf. 48 (1992) 763–780.